Non-physical Model of Lossy Transmission Line for Circuit Simulation of Segmented Traveling Wave Electroabsorption Modulators

K. Abedi[*a,b], V. Ahmadi[b], M. K. Moravvej-Farshi[b], M. H. Sheikhi[c] and F. Gity[b]

[a]Islamic Azad University, Ahar Branch.
[b]Dept. of Elect. Eng., Tarbiat Modares Univ., P. 0. Box 14155-4838, Tehran, Iran.
[c]Dept. of Electrical Engineering, Shiraz University, Shiraz, Iran.

***Abstract* — A HSPICE equivalent-circuit model for analyzing the frequency response of segmented traveling wave electroabsorption modulators (STEAM) is presented. The model is based on non-physical model for lossy transmission line. The analysis indicates that STEAM can achieve much wider bandwidth than the lumped electroabsorption modulator (LEAM) and TWEAM counterparts, with a small penalty in E/O conversion gain if low loss passive optical waveguide is available.**

***Index Terms* — circuit model, segmented traveling-wave electroabsorption modulators, LEAM, TWEAM**

I. INTRODUCTION

Electroabsorption modulators (EAMs) have been widely used in fiber optic communication systems for their small size, low driving voltage, low chirp, and high bandwidth [1,2]. In addition, due to matching of material systems, EAMs can be easily integrated with other optical components, such as semiconductor lasers, semiconductor optical amplifiers, and attenuators. Lumped-element EAM (LEAM) has achieved bandwidth as wide as 50 GHz [3]. The drawback is that its active waveguide has to be very short in order to achieve wide bandwidth, therefore substantial amount of E/O conversion gain is sacrificed. To achieve wide bandwidth with longer modulation length, traveling-wave EAMs (TWEAM) have been investigated in the recent years [1,2],[4,5], and 67 GHz has been achieved for $250\mu m$ long device [2]. The drawback of TWEAM is that it typically requires low-impedance termination, which again leads to penalty of modulation efficiency. Recently, segmented traveling-wave EAM (STEAM) has been experimentally investigated, with 95 GHz bandwidth extrapolated from the measured curve for a device with $210\mu m$ total active length [6]. The segmented traveling-wave employs a separate transmission line running parallel to the optical waveguide, as depicted in Fig.1. Modulation length (and its capacitance) in the optical waveguide is segmented and periodically connected to the transmission line as capacitive loading through the metal bridges, which lowers the microwave velocity and impedance.

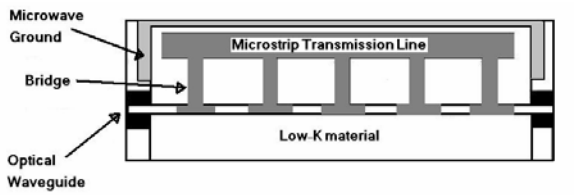

(a) Top view

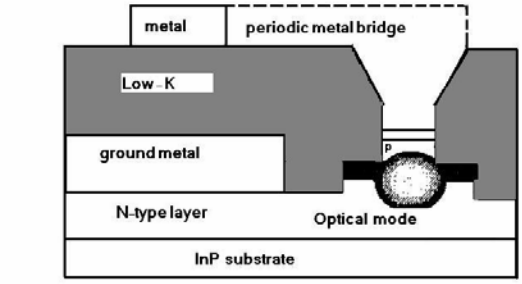

(b) Cross section view

Fig. 1. Schematic views of exemplary STEAM structure [7].

The design goals are to match the lowered microwave velocity with the optical group velocity, and match the lowered microwave impedance with 50Ω. In a STEAM, velocity matching and impedance can be achieved simultaneously; microwave loss can be very low since the transmission line separately designed [7]. Therefore, STEAM can potentially achieve very wide bandwidth.

In this paper, a HSPICE equivalent-circuit model of a segmented traveling-wave electroabsorption modulators is presented for the circuit level simulation of single device or Optoelectronics Integrated Circuit (OEIC) included modulators. Using this model, the frequency response of segmented TEAM is analyzed. The analysis indicates that STEAM can achieve much wider bandwidth than the LEAM and TWEAM counterparts,

* Corresponding author: k_abedi80@yahoo.com, phone: +98 21 88007395, Fax: +98-21-88006095

with a small penalty in E/O conversion gain if low loss passive optical waveguide is available.

II. CIRCUIT MODELING

From Lossless transmission line model, the microwave impedance and the microwave velocity index for the unloaded and loaded transmission lines can be calculated as:

Unloaded line:

$$Z_\mu = \sqrt{\frac{L_\mu}{C_\mu}} \quad , \qquad n_\mu = c\sqrt{L_\mu C_\mu} \tag{1}$$

loaded line:

$$Z_o = \sqrt{\frac{L_\mu}{(C_\mu + C_L)}} \quad , \quad n_o = c\sqrt{L_\mu (C_\mu + C_L)} \tag{2}$$

where L_μ and C_μ are the inductance and Capacitance per unit-length for the unloaded transmission line, C_L is the loaded capacitance per unit-length, c is the light velocity in vacuum. Z_μ and n_μ are the microwave impedance and phase velocity index values before loading, Z_o and n_o are the corresponding parameter values after loading. The traveling-wave design requires matching Z_o with $50\,\Omega$ and matching n_o with the optical group velocity index (~3.4 for InP waveguide). From (1) and (2) we can derive:

$$Z_\mu . n_\mu = Z_o . n_o \quad , \quad C_L = \frac{n_o^2 - n_\mu^2}{c . Z_o . n_o} \tag{3}$$

The above analysis indicates that simultaneous impedance matching and velocity matching can be achieved if the unloaded transmission line and the capacitive loading are designed to satisfy (3). Larger C_L is desirable to keep the device shorter, which can reduce the optical loss and enhance the modulation bandwidth. From (3), n_μ should be as small as possible to improve C_L. This requires the unloaded transmission line to have a fast microwave velocity [7]. The above analysis provides a rough guideline for the segmented traveling-wave electrode design, but it is not sufficient for estimating the modulation frequency response. The frequency response of a segmented traveling-wave modulator is limited not only by the impedance mismatch and the velocity mismatch, but also by the microwave loss, the microwave dispersion and filtering effects due to the periodic capacitive loading, and various parasitic effects. To analyze the frequency response including all these effects, we can use a microwave equivalent circuit model for the segmented traveling-wave electrode, as shown in Fig. 2 [8].

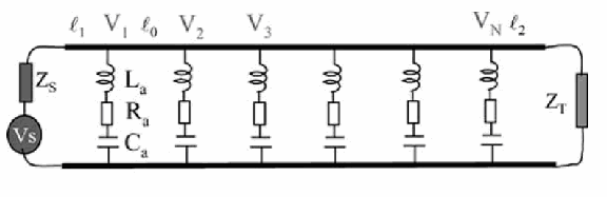

Fig. 2. Microwave equivalent circuit model for segmented traveling-wave optical modulators.

It represents a total of N segments of active modulation waveguide periodically shunting with a transmission line. Since each active segment is usually very short, it can be modeled by a lumped $L_a R_a C_a$ circuit. The inductance L_a is induced by the connection bridge; the resistance R_a includes the metal bridge resistance and the series resistance of the modulation waveguide; the capacitance C_a is the junction capacitance of the modulation waveguide. It is the voltage across the capacitance C_a that does the actual modulation. The microwave transmission line length between any two adjacent bridges is l_0. The microwave source impedance Z_s and the termination impedance are typically $50\,\Omega$. Under small-signal modulation, the modulation index for each active segment is linearly proportional to the modulation voltage across its capacitor C_a. The frequency response of the STEAM is therefore proportional to the square of the summation of modulation voltages across all the capacitors C_a multiplied by a phase factor caused by the traveling of the modulated optical wave envelope. The normalized frequency response of the STEAM is [8]:

$$M(f) = \left| \frac{2}{NVs} \sum_{n=1}^{N} VC_n e^{j\omega[l_1 + (n-1)l_0]/v_0} \right|^2 \tag{4}$$

Where VC_n is the modulation voltage across the nth capacitor, $\exp[j\omega(l_1 + (n-1)l_0)/v_o]$ is the microwave phase factor at the nth segment due to the traveling time of the modulated optical wave envelope, v_o is the optical group velocity in the optical waveguide and $\frac{NVs}{2}$ is the normalization constant for the summation of the voltage.

In this paper, we have used non-physical RLGC models to simulate transmission lines [9]. The non-physical RLGC models are based on the propagating wave analysis of transmission lines. Since the RLGC parameters derived by the propagating wave analysis are non-physical, they are categorized as 'nonphysical RLGC models. The advantage of using non-physical RLGC models is that it is easier to derive model parameters from measurements without any consideration on the transmission line structure.

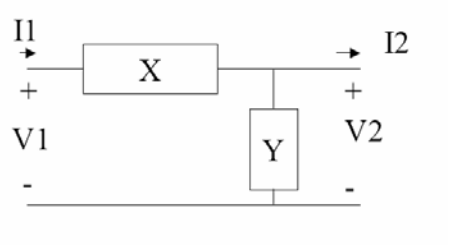

(a)

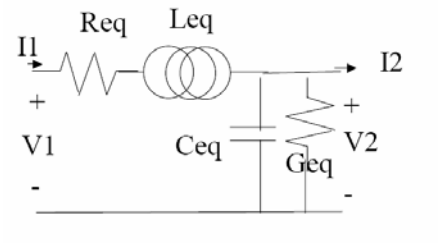

(b)

Fig. 3. RLGC model of the transmission line.

From [9], the non-physical RLGC parameters in Fig. 3 have the following parameters:

$$X = Z_\mu.\gamma \quad , \quad Y = \frac{\gamma}{Z_\mu} \qquad (5)$$

where Z_μ is the characteristic impedance, and γ is the propagation constant of the transmission line. The per unit-length RLGC parameters in Fig. 3(a) can be expressed as:

$$\mathrm{Re}\,q = \mathrm{Re}(X) \ , \ Leq = {\mathrm{Im}(X)}/{\omega} \ ,$$

$$Geq = \mathrm{Re}(Y) \quad , \quad Ceq = {\mathrm{Im}(Y)}/{\omega} \qquad (6)$$

The extraction of the non-physical RLGC model in (6) requires only two parameters, namely, the characteristic impedance and propagation constant, for constructing the RLGC circuit.

III. Estimation STEAM response

To simulate the transmission line in Fig. 1 in the frequency domain using the non physical RLGC model, the following parameters were used:

$Z_\mu = 80\Omega$, $\gamma = \alpha + j\beta$, $\alpha = 0.01 f^{1/2}$ mm^{-1} (f in GHz) , $\beta = \frac{2.pi.f}{c}.n_\mu$ and $l_2 = l_1 = l_0 = 0.1mm$

In exemplary STEAM, the total active modulation length is assumed to be $300\mu m$ divided into 6 segments. For each $50\mu m$ long active segment, we take $C_a \approx 45\,fF$, $R_a \approx 16\Omega$, $L_a \approx 30\,pH$ [7]. We first simulate the frequency response of the STEAM with target $Z_o = 33\Omega$. In this case the microstrip line and the optical waveguide of the STEAM have the same length of 1 mm, as derived from (3). The resulted 3-dB bandwidth is 72.8 GHz, as shown in Fig. 4.

Using the same waveguide design and $300\mu m$ total modulation length, we have also calculated the frequency response for the LEAM, and the result is plotted in Fig. 4. Only 25-GHz bandwidth can be achieved when the LEAM is terminated by 33Ω resistor. During the calculation for LEAM we assume $L_m = 0.58\,nH/mm$, $C_m = 0.93\,pF/mm$, $R_S = 0.75\Omega.mm$ [4].

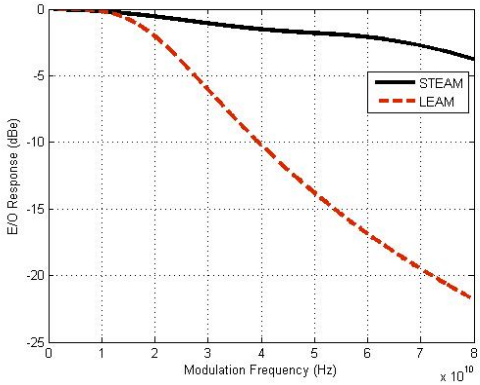

Fig. 4. Frequency responses for 1 mm long STEAM with 33Ω termination and 0.3 mm long LEAM with same resistor termination.

Fig. 5 shows the frequency responses of STEAMs designed to match with different terminator impedances. The following parameters have been used for the curves s1, s2, s3 and s4:

Curves1:

$RS = 33\Omega, RT = 33\Omega, Z_0 = 33\Omega, C_L = 285\ fF/mm, n_\mu = 1.4$

Curves2:

$RS = 50\Omega, RT = 33\Omega, Z_0 = 33\Omega, C_L = 285\ fF/mm, n_\mu = 1.4$

Curves3:

$RS = 50\Omega, RT = 50\Omega, Z_0 = 50\Omega, C_L = 138\ fF/mm, n_\mu = 2.13$

Curves4:

$RS = 50\Omega, RT = 33\Omega, Z_0 = 50\Omega, C_L = 285\ fF/mm, n_\mu = 2.13$

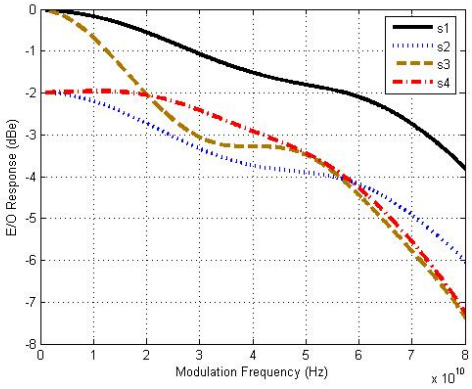

Fig. 5. Frequency responses for STEAMs using different terminator impedance Z_0

The penalty for the STEAM is some extra optical loss due to the passive optical waveguide. If the optical loss

in the passive optical waveguide is 2 dB/mm, the 0.7 mm long passive waveguide will add 1.4 dB optical losses to the STEAM, which converts to 2.8 dB compromise of E/O conversion gain.

IV. Conclusion

We have presented a HSPICE model based on non-physical RLGC for lossy transmission line of segmented traveling-wave electroabsorption modulators for analyzing the frequency response. The HSPICE analysis indicates that STEAM can achieve much wider bandwidth than the LEAM and TWEAM counterparts, with a small penalty in E/O conversion gain if lowloss passive optical waveguide is available.

References

[1] Y.-J. Chiu, H.-F. Chou, V. Kaman, P. Abraham, and J. E. Bowers, "High extincti ratio and saturation power traveling-wave electroabsorption modulator," *IEEE Photon. Technol. Lett.*, vol. 14, pp. 792–794, 2002.

[2] S. Irmscher, R. Lewén, and U. Eriksson, "InP/InGaAsP high-speed traveling-wave electro-absorption modulators with integrated termination resistors," *Photon.Technol. Lett.*, vol. 14, pp. 923–925, 2002.

[3] T. Ido, S. Tanaka, M. Suzuki, M. Koizumi, H. Sano, H. Inoue, "Ultra-high-speed multiple-quantum-well electroabsorption optical modulators with integrated waveguides," *Journal of Lightwave Technology*, vol.14, (no.9), p.2026-34. , 1996.

[4] G. L. Li, C. K. Sun, S. A. Pappert, W. X. Chen, and P. K. L. Yu, "Ultra high-speed traveling wave electroabsorption modulator: Design and analysis," *IEEE Trans. Microwave Theory Tech.*, vol. 47, pp. 1177–1783, 1999.

[5] G. L. Li, S. A. Pappert, P. Mages, C. K. Sun, W. S. C. Chang, and P. K. L. Yu, "High-saturation high-speed traveling-wave InGaAsP-InP electroabsorption modulator," *IEEE Photon. Technol. Lett.*, vol. 13, pp. 1076–1078, 2001.

[6] R. Lewén, S. Irmscher, U. Westergren, L. Thylén, and U. Eriksson, "Ultra High Speed Segmented Traveling Wave Electroabsorption Modulators," *Proc. Optical Fiber Communication (OFC'03)*, Atlanta, Georgia, Postdeadline paper PD38, 2003.

[7] G. L. Li, P. K. L. Yu, "Numerical modeling of segmented traveling-wave electroabsorption modulators," *IEEE MTT-S Int. Microwave Symp. Dig*, vol. 2, pp. 773 – 776, 2004.

[8] G. L. Li, T. G. B. Mason, P. K. L. Yu, "Analysis of Segmented Traveling-Wave Optical Modulators," *IEEE J. Lightwave Technol*, vol.22, p.1789-96, 2004.

[9] W. Kim and M. Swaminathan, "Validity of Non-Physical RLGC models for simulating Lossy Transmission lines", *AP-S 2002.*